Engineering Enzyme Subsite Specificity: Preparation, Kinetic Characterization, and X-ray Analysis at 2.0-Å Resolution of Val111Phe Site-Mutated Calf Chymosin[†]

P. Strop,[‡] J. Sedlacek,[§] J. Stys,[‡] Z. Kaderabkova,[‡] I. Blaha,[‡] L. Pavlickova,[‡] J. Pohl,[‡] M. Fabry,[§] V. Kostka,[‡] M. Newman,[⊥] C. Frazao,[⊥] A. Shearer,[⊥] I. J. Tickle,[⊥] and T. L. Blundell[*,⊥]

*Department of Biochemistry, Institute of Organic Chemistry and Biochemistry, Czechoslovak Academy of Sciences,
166 10 Prague 6, Czechoslovakia, Department of Gene Manipulations, Institute of Molecular Genetics, Czechoslovak Academy
of Sciences, 166 37 Prague 6, Czechoslovakia, and Laboratory of Molecular Biology, Department of Crystallography, Birkbeck
College, University of London, Malet Street, London WC1E 7HX, United Kingdom*

ABSTRACT: Comparison of the three-dimensional structure of bovine chymosin with the structures of homologous aspartic proteinases complexed with peptide inhibitors shows that Val111 in chymosin occupies a position between the specificity subsites S_1 and S_3. A mutation corresponding to Val111 to Phe has been introduced in an intermediary plasmid construct of prochymosin by bridging its unique restriction sites by a synthetic mutant oligonucleotide duplex. A prochymosin fusion product was expressed in *Escherichia coli* in such a way that the extension and substitution of the propart does not interfere with the activation of the zymogen. After activation of the crude prochymosin, the enzyme was purified by affinity chromatography on Sepharose with V-dL-P-F-F-V-dL as ligand. This procedure provided large amounts of pure protein as judged by FPLC, the activity/protein ratio, and SDS–PAGE. The enzymatic properties were determined by using a variety of peptide substrates and inhibitors; K_M values for the mutant enzyme were approximately twice those of the wild type, but the k_{cat} values were little changed. The mutant enzyme was crystallized, X-ray data were collected to 2.0-Å resolution by using a FAST area detector, and the structure was solved by using difference Fourier methods and refined to an *R* factor of 19.5%. The mutation leads to only local changes in conformation, with the phenylalanine side chain occupying part of the S_1 and S_3 pockets. This accounts for the increased K_M of this mutant for a substrate with a large phenylalanine side chain at P_1. It is also consistent with the higher affinity of the mutant for an inhibitor with small side chains at P_1 and P_3 when compared with the wild-type enzyme.

Bovine chymosin (E.C. 3.4.23.3) is an aspartic proteinase that is abundant in the fourth stomach of suckling calves (Foltmann, 1981). The active enzyme is formed from its zymogen, prochymosin, by proteolytic cleavage of the N-terminal 42-residue propeptide. Chymosin preferentially cleaves the milk protein κ-casein at a single Phe-Met bond with little nonspecific proteolysis, inducing instability in milk micelles, leading to clotting. This makes chymosin a commercially valuable enzyme in the production of cheese. Analogous proteolytic cleavage of other proteinacious materials such as soya may also be valuable in food processing.

The sequence of chymosin shows that it is homologous to pepsin and to other aspartic proteinases including kidney renin and microbial digestive proteinases such as penicillopepsin, endothiapepsin, rhizopuspepsin, and mucor-pusillus pepsin (Kostka, 1985). All have two aspartate residues (32 and 215 in pepsin numbering) that are essential for catalytic activity. Crystals were first obtained by Bunn et al. (1971), X-ray data at 3-Å resolution were collected by Blundell and Tickle (unpublished results), and these were used for solution of the rotation and translation functions by Safro et al. (1985) and Tickle (1985). The wild-type structure has been independently

solved and refined at 2.3-Å resolution by Gilliland et al. (1990) and at 2.2 Å by M. Newman, M. Safro, C. Frazao, G. Khan, A. Zdanov, J. J. Tickle, T. L. Blundell, and N. Andreeva (manuscript in preparation). These studies show that chymosin like other aspartic proteinases is a bilobal enzyme with a deep and extended substrate binding cleft. Each lobe is related by a pseudo 2-fold and contains approximately half the sequence folded in a similar way (Tang et al., 1978). The active site aspartates are situated at topologically equivalent positions, close together in the center of the active-site cleft. One lobe corresponds to a protomer of the retroviral aspartic proteinases (Miller et al., 1989; Lapatto et al., 1989).

During the past decade, heterologous expression of recombinant DNA prochymosin products has served two interconnected purposes. These are to establish an alternative source of this commericially important enzyme and to test ideas concerning the role of specific residues in prochymosin activation and chymosin activity. With respect to the latter, several site-specific mutations in the chymosin molecule and in the zymogen propart have been the reported (Suzuki et al., 1989; McCamman & Cummings, 1986, 1988; Mantafounis & Pitts, 1990) but none has allowed detailed structural as well as kinetic studies.

The specificity of chymosin is a consequence of the structure of the substrate-binding pockets. Although no three-dimensional structures of chymosin inhibitor complexes are available, the specificity pockets for peptide substrates may be identified by analogy with other aspartic proteinases such as endothiapepsin (Foundling et al., 1987; Blundell et al., 1987),

[*] To whom correspondence should be addressed.
[‡] Institute of Organic Chemistry and Biochemistry, Czechoslovak Academy of Sciences.
[§] Institute of Molecular Genetics, Czechoslovak Academy of Sciences.
[⊥] Birkbeck College, University of London.

penicillopepsin (James et al., 1982), and rhizopuspepsin (Bott et al. 1982; Suguna et al., 1987), for which there are high-resolution X-ray analyses of enzyme–inhibitor complexes. These studies have demonstrated the existence of well-defined specificity pockets S_4–S_3' (Schechter & Berger, 1967) that accommodate the side chains of the peptide substrate. The S_1 and S_3 subsites form two well-defined but contiguous pockets, which accommodate hydrophobic residues at P_1 and P_3 of the substrate. The S_1 position in chymosin is specific for a large hydrophobic side chain such as Phe. In the mammalian enzymes, residue 111 lies at the junction between S_1 and S_3. This position is occupied by a phenylalanine in pepsin but is substituted by a valine in chymosin. We hypothesized that this residue may play an important role in substrate recognition and in this paper seek evidence for this role.

We have studied both the three-dimensional structure and the catalytic properties of a site-directed chymosin mutant V111F, for which we predicted smaller S_1 and S_3 specificity pockets. We describe the application of an optimized over-production system for prochymosin (Sedlacek et al., 1987) and the use of plasmid constructs coding for the N-terminal fusion of five amino acids of the *Escherichia coli* β-galactosidase, seven amino acids of a polylinker, and prochymosin from its fifth amino acid. We show that the extension and substitution of the propart does not interfere with the activation of the zymogen. We describe the introduction of the mutation using a synthetic oligonucleotide duplex that bridges unique restriction sites, expression of the mutant, and affinity purification of the active enzyme. We describe and compare the catalytic properties and three-dimensional structures defined by X-ray analysis of the wild-type and mutant chymosins.

MATERIALS AND METHODS

Plasmids and Bacterial Strains. The expression plasmid, pMG13195, shown in Figure 1 was prepared as follows. The prochymosin cDNA (coding from its *Bam*HI site corresponding to the fifth amino acid of prochymosin) was first put in a *lac*-promoter-controlled pUC9-derived expression plasmid pMG424 and, then, together with the fused β-galactosidase and the polylinker segments, into tac-controlled construct pMG512 based on the pKK233-3 vector (a product of Pharmacia, Upsala). To increase pMG424, the segment of the P_{tac} transcription control and the region coding for the fusion prochymosin of pMG512 were rebuilt in the pUC series derived replicon, thus yielding an improved construct for expression of the wild-type product, pMG225. For the purpose of mutagenesis, the *Pst*-*Sal*I–*Bam*HI–*Sma*I–*Eco*RI linker sequence downstream of the prochymosin cDNA was replaced with a *Pst*I–*Hin*dIII-containing one, making the *Sma*I and *Eco*RI sites unique in the intermediary construct. The segment between the two sites was replaced by a duplex of the synthetic mutant 22-mer and 26-mer. The downstream linker of pMG225 was eventually shuttled back in the construction of pMG13195 (Figure 1).

The host strain, *E. coli* MT, was a hybrid of the parental strains of *E. coli* HB101:*recA* 13, *proA* 2, *rpsL* 20, and *E. coli* 71-18: δ-*proAB*, (F', *proAB*, LacI^q). The transfer of the F' element was achieved by the replica-mating technique by using proline-less solid medium supplemented with streptomycin for the hybrid selection. The *recA*– phenotype of *E. coli* MT and the F' presence in it were checked with the UV-sensitivity and the M13-phage-susceptibility tests, respectively, with the parental strains as controls.

Cultivation and Biomass Processing. E. coli MT cells harboring pMG13195 were grown at 37 °C in a medium containing tryptone, yeast extract, and lactose; aerobic cul-
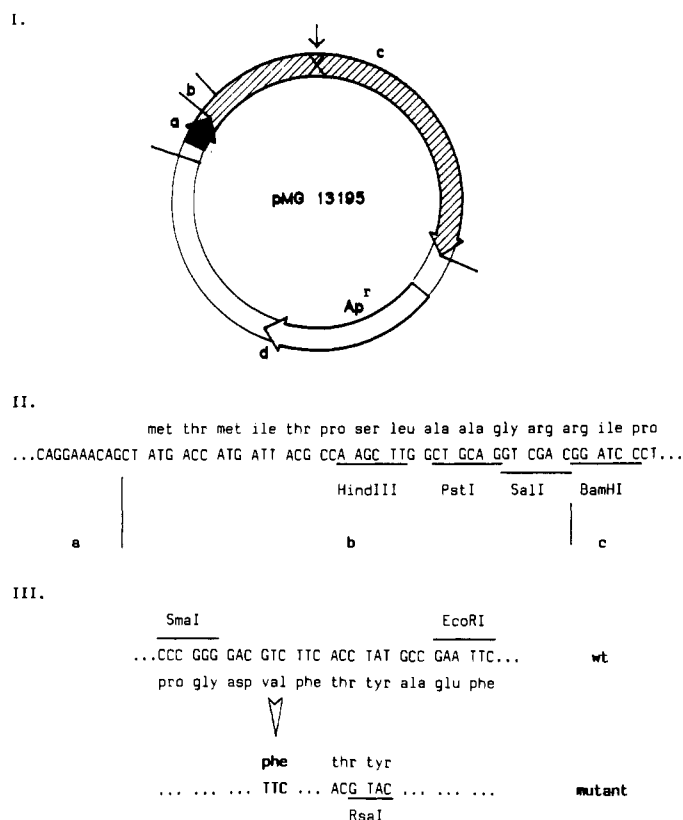

FIGURE 1: Expression plasmid pMG13195. (I) Segment map of the plasmid. The segment encoding *lac*–prochymosin fusion is shown by the hatched arrow. (a) pKK223-3-derived segment containing the *tac* promoter/operator (black arrow); (b) pUC9-derived portion of the *E. coli lacZ* gene and linker; (c) prochymosin cDNA starting from the 5th amino acid, the mutation (X) is indicated by an arrow; (d) pUC-series-derived rest of the vector part. (II) Sequences in the *lac* prochymosin fusion junction. The amino terminus of the expression product contains five amino acids of β-galactosidase plus seven polylinker-encoded amino acids fused to the 5th amino acid (Arg) of prochymosin. (III) Sequences in the mutated region of prochymosin. Val111 to Phe mutation is shown, as well as two silent mutations generating a new *Rsa*I site for screening of mutant clones (Sedlacek et al., 1987).

tivations used Erlenmayer flasks placed on a rotary shaker or a laboratory fermenter (Magnafem MA114, New Brunswick).

Formation of inclusions of the prochymosin product in the *E. coli* cells was quantitatively evaluated under a microscope in phase contrast by determining the diameter of an average inclusion body and calculating the volume V_1 of inclusions in 1 mL of the culture, the volume V_b of the cells present in 1 mL of the culture, and the ratio V_1/V_b.

In our expression system recombinant prochymosin is accumulated in inclusion bodies, which can fill up to 40% of cells (most typically around 25%). The isolation procedure of Marston et al. (1986) with minor modifications was used for the isolation of prochymosin from inclusion bodies.

Portions of 9–50 g of wet biomass were processed and the cell suspension was frozen and thawed before the lysozyme lysis step. The cell lysate was sonicated with a MSE Soniprep 150 to shear DNA and the urea-solubilized inclusions were dialyzed after the alkaline renaturation step in an Amicon DC 2 or in dialysis tubes against 8 mM Tris-HCl, pH 8.2. The batch DEAE-cellulose step was omitted and the fractions from the DEAE-cellulose column chromatography were analyzed for the content of the activatable prochymosin product by using the turbidimetric assay of McPhie (1976) with the milk substrate diluted in 20 mM sodium acetate, pH 5.6. Authentic calf chymosin served as the primary activity reference.

Isolation of Recombinant Mutant Calf Prochymosin from Inclusion Bodies and Purification by Affinity Chromatography. The method of Pohl et al. (1984), developed for purification of aspartic proteinases, was optimized for the isolation of recombinant chymosin. Pooled prochymosin fractions were activated to chymosin by a 30-min incubation at pH 3.0, in the presence of 0.2 M NaCl. A sample (400 mL) was then brought to pH 4.0 by the addition 0.5 M Tris buffer, pH 9.0, and 15% dioxane. The sediment formed was removed by filtration and the supernatant slowly applied to a 50-mL affinity column V-dL-P-F-F-V-dL-CH-Sepharose equilibrated with 0.03 M sodium formate buffer, pH 4.0, and 15% dioxane. The column was then washed with 200 mL of 0.03 M sodium formate buffer and 13% dioxane. The desorption of the bound chymosin was performed by 0.05 M sodium phosphate buffer and 1 mM EDTA, pH 6.5, with 25% of dioxane. Effluent was directly dropped into 2 volumes of the buffer 0.05 M phosphate, 1 mM EDTA, and 0.75 M NaCl, pH 5.7. Fractions were assayed for chymosin activity, pooled, and concentrated by using an Amicon YM 20 membrane.

The purity of the chymosin obtained from affinity chromatography was checked by FPLC (Mono Q 5/5 column, 0.05 M phosphate buffer, pH 6.5, 1 mM EDTA, 0.5 mL/min, linear gradient 0.75 M NaCl in 30 min), SDS electrophoresis (Laemmli, 1970), and amino acid analysis.

Synthesis of Substrates and Inhibitors. Substrates and inhibitors were prepared by solid-phase synthesis (Barany & Merrifield, 1979) as described elsewhere (Pavlickova et al., 1989), purified by reverse-phase HPLC, and characterized by amino acid analysis and FAB mass spectra. t-Boc phenylstatine 12 was prepared as described (Pavlickova et al., 1989). Amino acid analyses were performed on a Durrum 500 instrument. Mass spectra were obtained on a Finnigan machine.

Chicken pepsin activation peptide was prepared by activation of chicken pepsinogen.

Kinetic Measurements. Kinetic measurements were performed on a Cary 219 spectrophotometer in 0.1 M acetate or formate buffer, and 1 mM $CaCl_2$, 30 °C. Enzyme concentrations of 1.5–8 nM were used. The drop in the absorbancy at 305 nm was followed for the substrates with 4-nitrophenylalanine in the P_1' position. K_M and k_{cat} values were determined from plots of $1/v$ against $1/[S]$. Because it was not possible to find a tight-binding, specific inhibitor of chymosin to titrate the active enzyme, the k_{cat} values were based on the amount of the enzyme used in the assay, which was estimated from amino acid analysis.

The inhibition binding constants were obtained from both the IC 50 values and Dixon's plots $1/v$ against [I] (Dixon & Webb, 1979) by using a 5-min preincubation with the substrate K-P-L-E-F-F(NO_2)-R-L and 0.1% Brij 37. Other conditions used were similar to the substrate kinetics measurements described above.

Crystallization. Crystals suitable for X-ray analysis were grown by the method of microdialysis (McPherson, 1982) from a protein concentration of 10 mg/mL in 50 mM phosphate buffer at pH 5.6, containing 1 M NaCl (Bunn et al., 1971). After 1 week, the salt concentration was changed to 2 M NaCl. Crystals began to appear after about 4 weeks, and were fully grown by 2–3 months, reaching maximum dimensions of 0.6 × 0.6 × 0.3 mm. Crystals are of orthorhombic space group *I*222 or *I*2₁2₁2₁ with cell dimensions $a = 80.2$ Å, $b = 114.6$ Å, $c = 72.4$ Å, $\alpha = \beta = \gamma = 90°$. Within experimental error the cell dimensions of the mutant chymosin are the same as those of the wild type. The crystals contain one molecule per asymmetric unit, with a molecular weight of 35 700 (Foltmann

Table I: X-ray Data Collection and Processing Statistics

maximal resolution (Å)	2.0
no. of measurements	149 939
R_{merge}^a (%)	7.2
no. of unique reflections	22 098
measured/possible (%)	96.4
$I > 3\sigma(I)$ (%)	87.6

$^a R_{merge} = \sum(|I - \langle I \rangle|)/\sum I.$

et al., 1977).

X-ray Data Collection. X-ray intensity data were collected with a FAST electronic area detector diffractometer (Enraf Nonius, Delft), using a crystal to detector distance of 60 mm and a detector angle 23.5°. A 2.0-Å dataset was collected from one crystal by first rotating about *b** and then about axes ± 45° oblique to *b** to collect the cusp of reciprocal space. The reflection data (Table I) were evaluated on-line by using the program MADNES (Messerschmidt & Pflugrath, 1987). The data were corrected for absorption effects by using a semi-empirical transmission surface calculated from the transmission of the primary beam (G. Oliva, H. Driessen, and I. J. Tickle, unpublished data). The data were then divided into 3° batches about the rotation axis, and were scaled and merged by using the method of Fox and Holmes (1966) with a temperature factor relative to the first batch.

Refinement. The space group, *I*222, determined for the wild-type enzyme (Safro et al., 1985; Tickle, 1985) was assumed for the mutant crystals. With the wild-type observed data and phases derived from the refined crystal structure, an initial Fourier calculation was performed with coefficients $|F_{mutant}| - |F_{wild type}|$. The native data used in these calculations had been collected from several crystals to a resolution of 2.2 Å, containing 16 823 uniques with $R_{merge} = 8.9\%$ and 77.2% $> \sigma(F)$ and the structure was refined in our laboratory (M. Newman, M. Safro, C. Frazao, G. Khan, A. Zdanov, I. J. Tickle, T. L. Blundell, and N. Andreeva, manuscript in preparation) to an *R* factor of 17%. The difference map not only indicated the replacement of the valine at position 111 by phenylalanine but also a significant rearrangement of the adjacent residues that comprise the "flap" (Ser 72, Ile 73, His 74, Tyr 75, Gly 76, Thr 77, Gly 78, and Ser 79), a flexible type II' β-hairpin that lies above the active site and forms part of specificity pockets S_1 and S_2'. The validity of these changes was checked by calculating "omit maps", which confirmed the previously observed movements.

By use of the program FRODO (Jones, 1978) on an Evans and Sutherland PS300 interactive display graphics system, a phenylalanine side chain was inserted into the density at position 111. On the basis of the above difference and omit maps, it was apparent that the flap adopted two discrete conformations and thus both of these were modeled into the electron density. The resulting coordinates were used as the starting point for crystallographic refinement, using the least-squares refinement package RESTRAIN (Haneef et al., 1985), which applies pseudo-energy restraints to the molecular geometry. The program is implemented to run on the CRAY X-MP, so that one cycle of refinement at 2.0-Å resolution takes under 5 min of central processor time. Initially, rigid-body refinement was performed; this resulted in translations of the molecule by 0.116, 0.118, and 0.003 along the *a*, *b*, and *c*, axes respectively. The two possible conformations of the flap were subsequently refined with coupled occupancy.

After 33 cycles of positional refinement, including a number of cycles of individual temperature factor refinement, a $2|F_{obs}| - |F_{calc}|$ Fourier map was calculated with Sim-weighted coefficients (Read, 1986). This gave good density for most

Table II: Least-Squares Refinement Statistics

no. of protein atoms	2514
no. of solvent atoms	142
rms deviation from target values	
bond distances (Å)	0.022
bond angle distances (Å)	0.050
peptide bond planarity (Å)	0.019
resolution range (Å)	2.0–10
no. of unique refs used in refinement	21 710
R factor[a] (%)	19.5
mean B value for all atoms (Å^2)	30.3
estimated mean coordinate error[b] (Å)	0.27

[a] R factor = $\sum(||F_o| - |F_c||)/\sum|F_o|$. [b] Calculated by the method of Read (1986).

of the chymosin molecule and in addition showed electron density representing the mutant side chain.

The final R factor for 21 710 reflections between 2.0 and 10 Å with $F > 3\sigma(F)$ is 19.5%. One hundred forty-two waters have been included so far and individual B values have been refined. The final refinement characteristics are given in Table II. The refined coordinates have been deposited with the Protein Data Bank, Chemistry Department, Brookhaven National Laboratory, Upton, NY 11973, from which copies are available.

Inhibitor Modeling. In order to assess the effect of the site-directed mutation V111F on the kinetics of substrate proteolysis, it was necessary to obtain a model of the chymosin substrate transition-state complex. As there is no available high-resolution X-ray analysis of an inhibitor bound to chymosin, the three-dimensional structures of inhibitor complexes with the aspartic proteinase endothiapepsin were used to provide a basis for modeling a chymosin transition-state isostere complex.

By use of the program MNYFIT (Sutcliffe et al., 1987), the three-dimensional structures of endothiapepsin complexed with H261 (Veerapandian et al., 1990), H256 (Cooper et al., 1987), and CP69,799 (Sali et al., 1989) were least-squares fitted to the chymosin wild-type and mutant structures. In the mutant flap conformation B, where the side chain of Tyr 75 is directed toward Trp 39, the positions of the inhibitors were easily accommodated within the cleft of the chymosin molecule. However, for conformation A, the aromatic ring of Tyr 75 completely blocked off the entrance to specificity pocket S$_1$, thus preventing a large substrate side chain (i.e., Phe) at P$_1$ from binding in this pocket. Thus conformation B was used in subsequent modeling. The consensus inhibitor conformation was used to guide the modeling of a transition state for the sequence of the substrate K-P-L-E-F-F(NO$_2$)-R-L, which had been used in the kinetic measurements. Hydrogen bonds that were conserved between the three inhibitors and endothiapepsin were modeled into the chymosin–substrate complex. The conformation was optimized for steric interactions between enzyme and substrate.

RESULTS AND DISCUSSION

The Prochymosin Product Accumulation and Recovery. The *E. coli* MT cells, which harbor plasmid pMG13195 (Figure 1) coding for the V111F mutated fusion calf prochymosin, form cytoplasmic inclusions of the recombinant product. The entire population of the cells in the induced cultures contained the inclusions and their partial volume [V_i/V_b] evaluated by microscopy was about 30%. The processing of the isolated and washed inclusions by a slightly modified procedure of Marston et al. (1986) enabled recovery of the activatable prochymosin product with yields of about 1 mg per gram of wet biomass (in enzyme activity terms) after
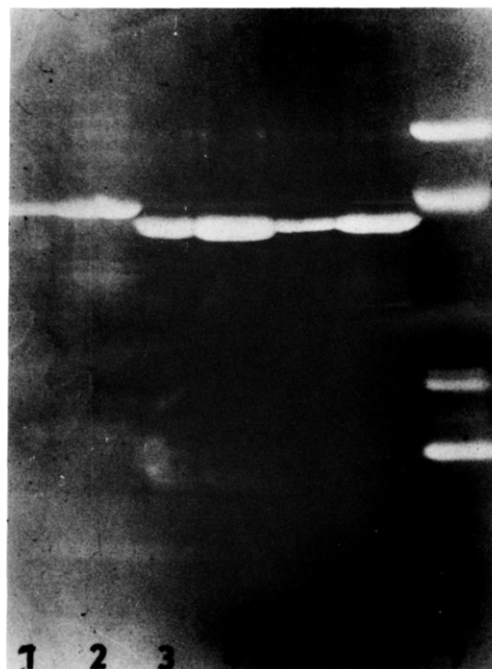

FIGURE 2: SDS electrophoresis of recombinant calf prochymosin and chymosin. Lanes 1 and 2, prochymosin accumulated in inclusion bodies (2 and 10 μg, respectively); lanes 3–6, chymosin after activation of prochymosin from inclusion bodies (2 and 10 μg); lane 7, molecular weight markers 67K, 43K, 21K, and 14K.
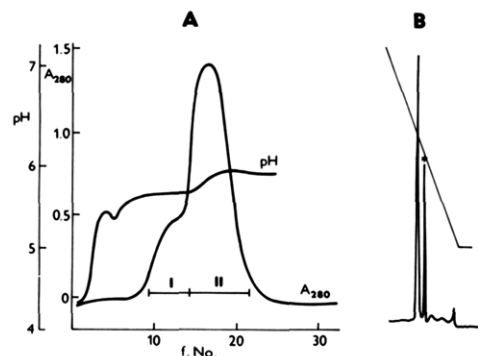

FIGURE 3: Affinity chromatography and FPLC ion-exchange analysis of recombinant mutant Val111 to Phe chymosin. (A) Absorbancy and pH profile for desorption of chymosin from V-dL-P-F-F-V-dL-CH-Sepharose column. Pooled fractions II were used for further studies. For conditions, see Methods. (B) FPLC analysis of fraction II on Mono Q 5/5 column (Pharmacia), 0.05 M phosphate buffer, pH 6.5, linear gradient of 0–1.3 M NaCl during 30 min, 1mL/min, 280 nm, 0.5 AUFS. *, artifact from sample buffer.

the DEAE-cellulose chromatography step. The yields were systematically somewhat higher with biomass from flask cultivations than from those from the fermenter. The expression capacity of pMG13105 appeared to be the same as that of the parental wild-type pMG225 and no effect on the codon substitutions was observed (one new codon was introduced for the mutation; the other two changes were silent but introduced a reference restriction site).

Purification. The mutant prochymosin that had been purified on the DEAE-cellulose was little contaminated by other proteins and was fully convertible to enzyme as shown in Figure 2.

Correctly folded recombinant V111F chymosin was purified from inclusion bodies by use of an affinity column comprising the weak inhibitor V-dL-P-F-F-V-dL bound to CH-Sepharose (Figure 3). Active mutant chymosin was eluted in two close peaks (I and II) due most probably to the pH gradient profile formed after application of buffer at pH 6.5. Both peaks

Table III: Comparison of K_M and k_{cat} Values Determined for Wild-Type and V111F Mutant Chymosin by Using a Variety of Peptide Substrates (I–IV)[a]

substrate[b]			wild type			mutant		
P_1	P_1'	pH	K_M (mM)	k_{cat} (s^{-1})	k_{cat}/K_M (mM^{-1} s^{-1})	K_M (mM)	k_{cat} (s^{-1})	k_{cat}/K_M (mM^{-1} s^{-1})
I	H-P-H-L-S-F	F*-R-I-P-P-K-K	5.6	0.028	22.5	804	0.053	20	377
			4.5	0.091	35	385		n.d.	
			3.1	0.12	0.19	1.58	app.1	0.14	
II	P-H-L-S-F	F*-R-I-P-P-K	5.6	0.083	29	349	0.33	8.9	26.9
			3.1	0.25	3.3	13.2		nd.	
III	H-P-H-P-L-S-F*	M-A-I-P-P-K-K	5.6	0.145	87	600	0.257	85	330
			3.1	0.53	1.19	2.25	app.1	2.4	
IV	K-P-L-E-F	F*-R-L	5.6	0.051	24.3	476	0.139	22	155
			3.1	0.25	50	200	0.5	71	143

[a] Conditions were 0.1 M acetate or formate buffer, 1 mM $CaCl_2$, 30 °C, enzyme concentration 1.5–8 nM. For other conditions see Methods. [b] The * indicates that the residue occupying this position in the substrate is 4-nitrophenylalanine.

showed the same milk clotting activity. Peak II was used in kinetic measurements and crystallization experiments. By use of the isolation protocol described in Methods a recovery of over 90% of the activity of chymosin was achieved. Chymosin obtained from the affinity column was pure as judged by FPLC MONO Q chromatography (Figure 3), SDS electrophoresis, and amino acid analysis.

Kinetic Measurements. The kinetic measurements of the wild-type and Val111 to Phe chymosins were compared by using the set of substrates listed in Table III. Substrates I–III are based on the cleaved sequence of κ-casein (Jolles et al., 1968; Mercier et al., 1973) and substrate IV was found earlier to be a convenient substrate for chymosin and other aspartic proteinases of animal or microbial origin (Dunn et al., 1986, 1987). The best or most convenient two substrates for wild-type chymosin were I and IV, giving K_M values of 0.028 and 0.051 mM, respectively, and k_{cat} values of approximately 20 s^{-1} each at pH 5.6. Both substrates followed the Michaelis–Menten kinetics and showed a linear dependence of the initial rate of cleavage on the concentration of the enzyme, as well as linear $1/v$ versus $1/[S]$ plots. This is in agreement with Visser, who exhaustively investigated the K_M and k_{cat} values for a large set of similar substrates spanning the sequence of κ-casein from residue 98–112 and found similar values for peptides of the size of peptides I–III shown in Table III (Visser et al., 1987).

It is generally observed that the k_{cat} is approximately equal in the wild-type and mutant enzymes, indicating that the mutation Val111 to Phe has not affected the catalytic activity of chymosin. However, in all substrates, the value of k_{cat}/K_m decreases for the mutant, resulting mainly from an increase in K_M.

A series of inhibitors was also compared at pH 4.5–5.6 for both wild-type and mutant chymosin (Table IV). The peptide V-dL-P-F-F-V-dL (inhibitor I), which was used as a ligand for the affinity chromatography, is not bound very strongly to either enzyme. Its K_I of 0.2 mM is comparable to the K_M value of substrate III. Iva pepstatin (inhibitor II), which has an aliphatic leucine-like side chain in position P_1, is bound slightly better to the mutant enzyme (K_I is 1.6 × 10^{-5} M). The inhibitor H-L-S-PheSta-A-C designed for chymosin with the benzyl side chain in position P_1 is bound over two times less tightly to the mutant (K_I is 2.8 × 10^{-6} M).

X-ray Analysis. The method described has allowed the determination of the mutant chymosin structure. For the most of the molecule, the electron density is of high quality and allows unambiguous assignment of the main chain and side chain atoms. With transformation of the wild type onto the mutant structure to minimize the overall difference, the rms deviation between all coordinates common to the mutant and

Table IV: Comparison of K_I Values Determined for Wild-Type and V111F Mutant Chymosin by Using a Variety of Peptide Inhibitors (I–IV)[a]

	inhibitor	pH	K_I (μM) wild type	K_I (μM) mutant
I	V-dL-P-F-F-V-dL	4.5	200	200
II	Iva pepstatin[b]	4.5	20	16
III	H-L-S-PheSta[c]-A-C	4.5	1.05	2.80
IV	CP-propart P1-P42[d]	5.6	0.08	0.23

[a] The K_I values were obtained from IC$_{50}$ values with 0.25 mM peptide K-P-L-E-F-F(NO$_2$)-R-L in the presence of 0.1% Brij. For other conditions, see Methods. [b] Iva pepstatin is Iva-Val-Val-Sta-Ala-StaOMe. Iva is isovaleric acid, i.e., 3-methylbutanoic acid (valine with no amino terminus); Sta is statine, i.e., 4-(S)-amino-3-(S)-hydroxy-6-methylheptanoic acid. [c] PheSta is phenylalaninestatine, i.e., 4-(S)-amino-3-(S)-hydroxy-5-phenylpentanoic acid. [d] CP-propart P1-P42 is chicken pepsinogen propart activation peptide residues P1-P42.

wild-type enzyme structures is 0.63 Å. (This comparison excludes the residues corresponding to the "flap".) For the C_α coordinates the rms diffrences is 0.27 Å. Although these values are somewhat larger than the estimated coordinate error (Table II), the majority of the difference is contributed by the poorly defined surface loops. Thus the rms difference for atoms, excluding the flap, within a 10-Å sphere of 111 C_α is 0.32 Å for all atoms and 0.29 Å for C_α positions, a value comparable with the coordinate error.

Figure 4 shows the $2|F_{obs}| - |F_{calc}|$ electron density corresponding to Phe 111 in the mutant structure, confirming that the side chain of 111 occupies a position between specificity pockets S_3 and S_1. No local conformational change of the main chain of 111 is indicated. In comparison with the adjacent phenylalanine at 112, the density is not as well formed. The average B value for the side chain of Phe 111 is 42 Å^2, significantly above the mean. The mutated residue is situated on the edge of specificity pocket S_1, with a large solvent-accessible surface area (Table V), suggesting that this side chain is allowed a high degree of movement. This is confirmed by a comparison of Phe 111 from porcine pepsin (Cooper et al., 1990), occurring in an identical position. It has an average side chain B value of 43 Å^2, which is almost exactly equal to that in mutant chymosin. Other residues that are also involved in specificity pocket S_1 are shown in Figure 4, indicating the hydrophobic nature of this pocket. Excluding the flap, all residues that contribute to S_1 are well defined in the $2|F_{obs}| - |F_{calc}|$ density map.

The $|F_{V111F}| - |F_{wild type}|$ difference map indicated that residues 74–79 comprising the flap underwent a significant rearrangement in the V111F structure. On the basis of this map and subsequent omit maps, residues 72–79 were refined in two different conformations (A and B) with coupled occupancies.
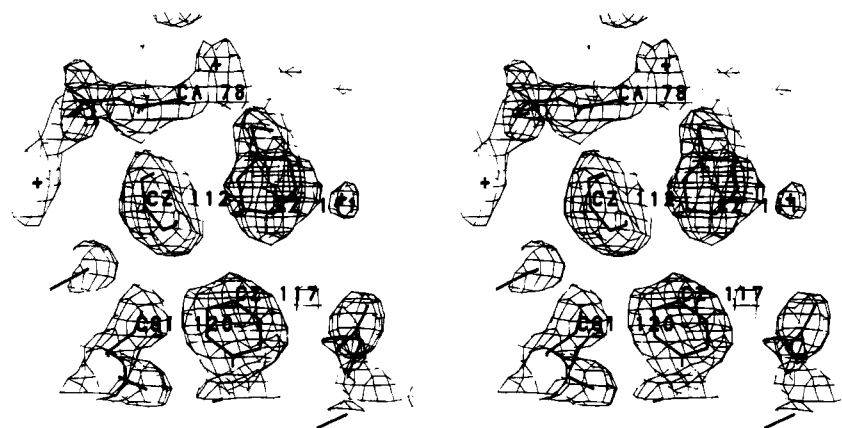
FIGURE 4: Final weighted $2|F_{obs}| - |F_{calc}|$ electron density corresponding to the mutated residue Phe 111 contoured at 1 σ. The densities for other hydrophobic residues Phe112, Phe117, and Ile120 that form part of specificity pocket S_1 are also indicated.
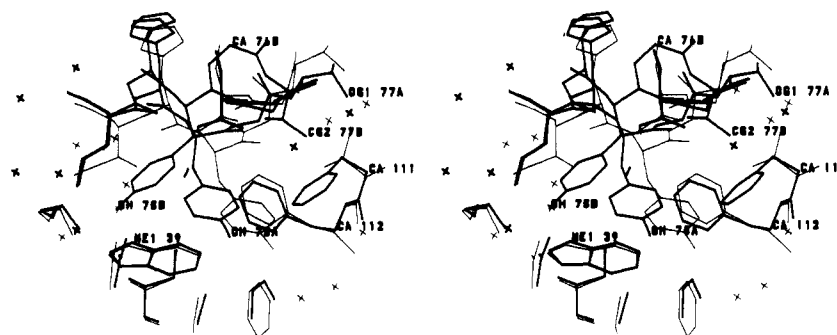

FIGURE 5: Two-flap conformations A and B in the mutant, superimposed on the wild-type structure. Bold lines show the mutant; thin lines show the wild-type enzyme. The two conformations are represented by letters (A or B) after the residue number.

Table V: List of Protein Contacts Made by Side Chain at Position 111 in V111F Chymosin, Wild-Type Chymosin, and Porcine Pepsin

enzyme structure[a]	residues within 4-Å cutoff criteria	no. of contacts[b]			accessibility[c] ($Å^2$)
		all atoms	C	N and O	
V111F flap A (Phe111)	Tyr75-Thr77-Asp110-Phe112	19	14	5	60
V111F flap B (Phe111)	Thr77-Asp110-Phe112	16	13	3	81
W-T chym[d] (Val111)	Tyr75-Thr77-Gly78-Asp110-Phe112	7	2	5	43
P.pepsin[e] (Phe111)	Thr77-Ser110-Leu112-Ala115-Phe117	12	9	3	84

[a] Residues in brackets indicate the amino acid occupying position 111. [b] The number of contacts was calculated by using a 4.0-Å cutoff distance. [c] Solvent-accessible surface area of residue 111 was calculated in $Å^2$ by using the method of Kabsch and Sander (1983). [d] Wild-type chymosin. Residues 72–79 occupy a position that is analogous to the flap conformation A in the mutant structure. Extra contacts are made with Gly78 due to the presence of a β-methyl group on Val 111. [e] Porcine pepsin. The flap takes the more usual conformation B with a similar class of contacts to V111F flap B. Extra contacts are made with Ala115 and Phe117.

At the end of the refinement, $Occu_A = 0.40$ and $Occu_B = 0.60$, with the *B* values for the two positions being 36 and 37 $Å^2$, respectively. Although the density for neither A nor B is continuous for the main chain between C 75 and C_α 76, the density for B is far superior. Thus, it appears that conformation B is significantly more highly populated than A.

The two flap positions take remarkably different conformations (Figure 5), the largest movements involving the conserved side chain of Tyr 75, which forms part of subsite S_1 and may play a role in stabilizing the substrate tetrahedral intermediate. In conformation A, the side chain of Tyr 75 is in a position analogous to wild-type chymosin (Gilliland et al., 1990; M. Newman, M. Safro, C. Frazao, G. Khan, A. Zdanov, I. J. Tickle, T. L. Blundell, and N. Andreeva, manuscript in preparation) where it takes a trans conformation pointing out into the substrate binding cleft, hydrogen bonding to the carbonyl of Gly 217. In this position it partially blocks off the entrance to specificity pocket S_1, as indicated by the lower accessible surface area of 111 (Table V). However, in position B, the Tyr 75 side chain takes a gauche + conformation, rotating by roughly 124° about the C_α–C_β bond so that its OH

group hydrogen bonds to Trp 39 NE1 at a distance of 2.96 Å, as it does in the crystallographic structures of porcine pepsin and the fungal aspartic proteinases. To accommodate this movement of the tyrosine side chain, residues 74B to 76B move away from the enzyme by approximately 2 Å. Although the main chain torsion angles in flap B differ from those in porcine pepsin, the overall trace of the main chain is remarkably similar between the two mammalian enzymes.

Table V shows that the side chain of 111 makes multiple contacts with the residues that comprise the flap and that these contacts differ between the wild-type and mutant structures. Thus it is probable that the rearrangement of the flap is caused by the mutation of residue 111, in conjunction with the effect of the crystal environment. Specifically, the occurrence of close contacts of approximately 3 Å between Thr 77, Ser 79, and a symmetry-related molecule restricts the movement of the flap. In the wild-type enzyme, this results in an unfavorable steric interaction in conformation B. This can only be relieved by a rearrangement of residues 74–77 to produce conformation A. However, due to the insertion of a large aromatic group in the mutant, conformation B is preferred due to the improved

Table VI: Sequence Alignment Based on the 3-D Superposition of Aspartic Proteinase Structures in the Region of the α-Helix 110–114 (Pepsin Numbering)[a]

| | residue no. | | | | | | | | | | | | | | | | | | | |
	100										110									118
w-t chym	T	V	G	L	S	T	Q	E	P	G	D	V	F	T	Y	A		E	F	D
V111F chym	T	V	G	L	S	T	Q	E	P	G	D	F	F	T	Y	A		E	F	D
porcine pepsin	I	F	G	L	S	E	T	E	P	G	S	F	L	Y	Y	A		P	F	D
endothiapepsin	A	V	E	S	A	K	K	V	s	s	S	F	t	e	d		s	T	I	D
penicillopepsin	A	V	Q	A	A	Q	Q	I	S	a	Q	F	q	q	d		t	N	N	D
rhizopuspepsin	T	I	E	L	A	K	R	E	a	a	S	F	A	S	G			P	N	D

[a] All comparison are performed in a pairwise manner with wild-type chymosin by using MNYFIT (Sutcliffe et al., 1987). Residues that do not align with a 3.5-Å cutoff distance are displayed in lower case. The standard one-letter amino acid code is used.

packing for the Tyr 75 side chain. In solution with the absence of crystal packing forces, it is probable that both the wild type and the mutant have the usual conformation B found in other aspartic proteinases.

The detailed positions of the residues in conformation A of the mutant differ slightly from the wild-type enzyme (Figure 5). The absence in the mutant of valine's γ-methyl at residue 111 removes contacts with Thr 77 and Gly 78 and enables the flap to move 0.5 Å toward residue 111. Also, the presence of a more bulky aromatic group at 111 displaces the side chain of flap A Tyr 75 by approximately 2 Å relative to wild-type chymosin (Figure 5). The combination of the above effects results in a slight twist between the wild-type flap and mutant flap A. Table V indicates that Phe 111 in the mutant structure makes a greater number of contacts than either wild-type chymosin and porcine pepsin. This is due to the close proximity of 111 to the adjacent phenylalanine side chain at 112, forming an edge-to-ring-f ace interaction as described by Singh and Thornton (1985).

As in all other aspartic proteinases defined by X-ray analysis, residues in the region of 110–114 form an α-helix in both wild-type and mutant chymosins. The χ_1 torsion angle for the Phe 111 side chain is 179°, corresponding to one of two preferred torsion angles for phenylalanine residues in α-helices (McGregor et al., 1987). This is similar to the value for Phe 111 in porcine pepsin of 172°. However, there is a difference between the χ_2 value of 69° for mutant chymosin and the equivalent value in porcine pepsin of 140°. This change is most likely due to the close contacts with Thr 77 in the mutant. There is no evidence that the existence of two conformations of the flap have resulted in two conformations of the mutated residue.

The three-dimensional structure of the chymosin mutant implies a change in the usually accepted sequence alignment in the region of the mutation. Table VI shows that in endothiapepsin and penicillopepsin there appears to have been an insertion at the C-terminus of the turn of helix 111–114 and a deletion at the N-terminus. Rhizopuspepsin appears only to have the deletion at the N-terminus. The helices have not changed in relative positions, but the connecting loops have altered in length. Such an insertion and deletion had been considered previously in modeling studies of chymosin and renin (Sibanda et al., 1984). The new alignment shows that Val 111 in wild-type chymosin aligns with a phenylalanine in pepsin but a serine in endothiapepsin.

Substrate/Inhibitor Interactions and Enzyme Specificity. As the flap conformation A appears to be a consequence of crystal packing leading to a destabilization of the more usual conformation B and because the orientation of Tyr 75 in flap conformation A is not compatible with a productive mode of binding, it was assumed that, in solution, a bound substrate would only occur with conformation B. Thus flap B was used in both the wild-type and mutant complex models. Figure 6a shows the conformation of the substrate transition state isostere

Table VII: List of Protein Contacts Made by Side Chains at Positions P_1 and P_3 of Substrate IV [K-P-L-E-F-F(NO_2)-R-L] in Wild-Type and V111F Chymosin Complex Models

substrate side chain	enzyme structure	residues within 4-Å cutoff criteria	no. of contacts[a]		
			all atoms	C	N and O
P_1(Phe)	w-t chym	Leu30-Asp32-Tyr75-Phe117-Gly217	14	9	5
P_1(Phe)	V111F	Leu30-Asp32-Tyr75-Thr77-Phe111 Phe112-Phe117-Ile120-Gly217	21	17	4
P_3(Leu)	w-t chym	Gln13-Phe117-Ser219	5	3	2
P_3(Leu)	V111F	Ser12-Gln13-Phe111-Phe117-Ser219	12	7	5

[a] The number of contacts made by substrate side chains at positions P_1 and P_3 was calculated by using a 4.0-Å cutoff distance.

for the sequence K-P-L-E-F-F(NO_2)-R-L bound to the chymosin's specificity pockets S_3 and S_1, and Figure 6b shows a similar view for the mutant. It is apparent that the mutant side chain Phe 111 occupies a position between the substrate side chains P_3 and P_1. Thus, whereas in the wild-type enzyme both these side chains are easily accommodated, in the mutant enzyme the size of these pockets is reduced, and some rearrangement of both P_3 and P_1 side chains is necessary to reduce unfavorable van der Waals' contacts. Table VII lists the contacts made by the side chains at P_3 and P_1, which define the pockets S_3 and S_1, respectively. For both P_3 and P_1, the number of contacts has increased in the mutant enzyme, indicating the reduced volume of the pockets. In S_1, the phenylalanine side chain of the substrate make contacts <3.1 Å with 75 and 111 and, in S_3, the leucine side chain <3.2 Å from 13 and 111. These show that whereas the wild type can accommodate P_1(Phe) and P_3(Leu), these are less easily accommodated in the mutant and tight binding would require some small rearrangement of the residues in those pockets.

The kinetic data (Table III) are consistent with the proposition that the mutation of valine to the larger phenylalanine at position 111 on the edge of the primary S_1 and secondary S_3 binding pockets would decrease the binding of substrate with bulky residues in position P_1 and P_3. Indeed, the wild-type chymosin displayed tighter binding (lower K_M values) for all the peptides with phenylalanine or *p*-nitrophenylalanine at P_1 and a leucine at P_3 both at pH 5.6 and at pH 3.7. The K_M values for the mutants are approximately two or three times higher, with k_{cat} little changed. Similar changes in K_M were recently reported for an identical chymosin mutant with the peptides K-P-I-E-F-F(NO_2)-R-L and L-S-F(NO_2)-NLe-A-L (Suzuki et al., 1989). However, larger changes in the value of k_{cat} were reported; these may be ascribed to differences in the assay or the use of pseudochymosin (Pedersen et al., 1979), which retains part of the propeptide on acid activation at pH 2.3.

The results of the inhibitor binding studies are summarized in Table IV. Inhibitor I, which was used in the affinity
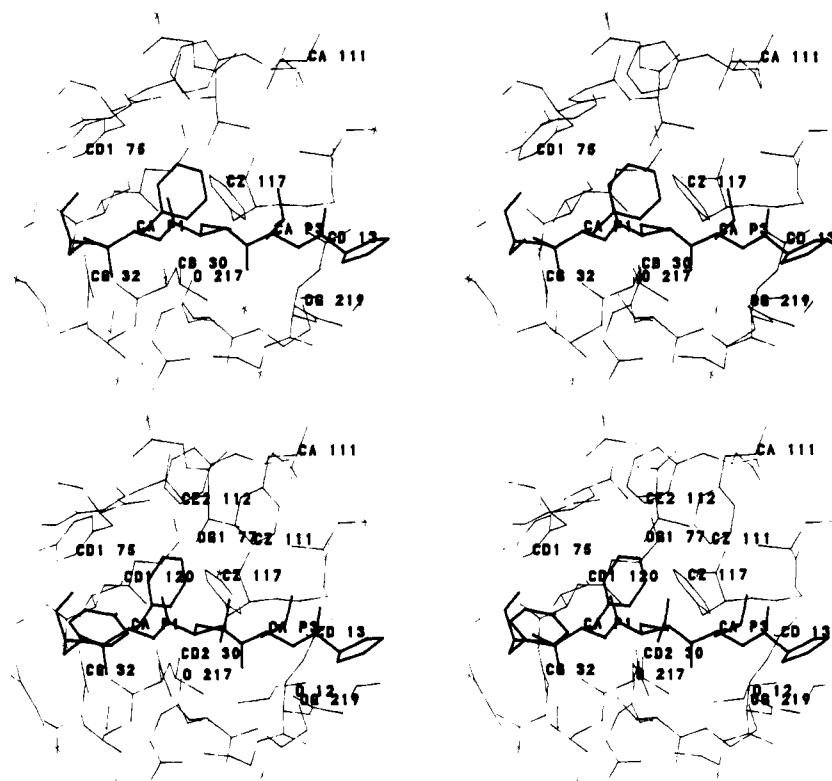
FIGURE 6: Model of substrate IV [K-P-L-E-F-F(NO$_2$)-R-L] transition-state complex with (a, top) wild-type and (b, bottom) mutant chymosin, showing the binding pockets S$_1$ and S$_3$. Note that the flap residues assume conformation B in both models. Residues P$_4$-P$_1'$ of the substrate are shown in bold lines, the enzyme in thin lines. The positions of Leu P$_3$ and Phe P$_1$ of the substrate ar indicated, as well as 111 of the enzyme. All other residues labeled contact either P$_3$ or P$_1$ side chains with a cutoff distance of 4.0 Å (see Table VII).

chromatography, is the weakest bound of all four inhibitors and displays no change in K_I for the mutant enzyme. Although the most probable mode of the binding of this inhibitor is with the two phenylalanine residues occupying the S$_1$ and S$_1'$ pockets, the presence of the dL at positions P$_3$ and P$_3'$ would need alternative binding in S$_3$ and S$_3'$ in both the wild type and the mutant, disrupting the usual hydrogen bonding between the inhibitor (Foundling et al., 1987) and the enzyme. This is likely to decrease the binding at S$_1$ and S$_1'$ and make the Val to Phe mutation of less importance. This is consistent with the fact that this inhibitor is bound 2 orders of magnitude weaker than transition-state analogues, such as pepstatin- or statine-containing inhibitors (inhibitors II and III), which also contain the tetrahedral hydroxyl group hydrogen bonded between the two catalytically active carboxylates (Foundling et al., 1987). As this is an inhibitor rather than a substrate, it is likely that the P$_1$-P$_1'$ peptide does not approach the catalytic residues closely enough to effect cleavage.

Inhibitor II shows an increase in binding in the mutant structure. This is most likely due to the fact that the smaller side chains at P$_3$(Val) and P$_1$(Leu) are more favorably accommodated in the smaller binding pockets S$_3$ and S$_1$ of the mutant enzyme. Inhibitor III with the larger side chains P$_3$(Leu) and P$_1$(Phe) is bound less strongly to the mutant.

There is very little known about the mode of binding of the activation peptide from chicken pepsinogen P1-P42, which is a long and largely basic polypeptide. The binding of this peptide to chicken pepsin is strongly influenced by pH and ionic strength. Therefore it is believed that the charge interactions play a dominant role (Pohl et al., 1985). Surprisingly this polypeptide is a strong inhibitor of the chymosin as well ($K_I = 8 \times 10^{-8}$ M). The binding of this peptide by the mutant is approximately 3 times weaker ($K_I = 2.3 \times 10^{-7}$ M). There are only three aromatic residues. The sequence around Phe 26 fits well to the known specificity of chymosin.

Therefore it is possible that Phe 26 is bound in the S$_1$ pocket and the binding by the mutant is weaker due to steric hindrance with the side chain of Phe 111.

This study is consistent with the proposition that substitution of Val111 (pepsin numbering) of chymosin by phenylalanine reduces the size of the S$_1$ and S$_3$ specificity pockets. Site-directed mutagenesis and X-ray analysis have shown that the valine may be replaced by a phenylalanine with little perturbation of the structure of the chymosin molecule as a whole. However, considerable rearrangement occurs in the "flap" residues as a consequence of the substitution at position 111 and the crystal environment. The mutation decreases the specificity (k_{cat}/K_M) toward substrates with a large residue at P$_1$. It increases binding of inhibitors with smaller side chains at P$_1$ and P$_3$ but decreases binding when P$_1$ and P$_3$ are larger. Such a study illustrates the value of a multidisciplinary protein engineering cycle in the design of enzymes with changed specificity at a particular subsite in the substrate molecule.

REFERENCES

Barany, G., & Merrifield, R. B. (1979) in *The Peptides*:

Analysis, Synthesis and Biology (Gross, E., & Meienhofer, J., Eds.) pp 1–228, Academic, New York.

Blundell, T. L., Cooper, J., Foundling, S. I., Jones, D. M., Atrash, B., & Szelke, M. (1987) *Biochemistry 22*, 5585–5590.

Bott, R. R., Subramanian, E., & Davies, D. R. (1982) *Biochemistry 21*, 6956–6962.

Bunn, C. W., Moews, P. C., & Baumber, M. E. (1971) *Proc. R. Soc. London, B 178*, 245–258.

Cooper, J., Foundling, S., Hemmings, A., Blundell, T. L., Jones, D. M., Hallet, A., & Szelke, M. (1987) *Eur. J. Biochem. 169*, 215–221.

Cooper, J. B., Khan, G., Taylor, G., Tickle, I. J., & Blundell, T. L. (1990) *J. Mol. Biol. 214*, 199–222.

Dixon, M., & Webb, E. C. (1979) *Enzymes*, 3rd ed., Academic, New York.

Dunn, B. M., Jiminez, M., Parten, B. F., Valler, M. J., Rolph, C. E., & Kay, J. (1986) *Biochem. J. 237*, 899–906.

Dunn, B. M., Valler, M. J., Rolph, C. E., Foundling, S. I., Jimenez, M., & Kay, J. (1987) *Biochim. Biophys. Acta 913*, 122–130.

Foltmann, B. (1981) *Essays Biochem. 17*, 52–84.

Foltmann, B., Pedersen, V. B., Jacobsen, H., Kauffman, D., & Wybrandt, G. (1977) *Proc. Natl. Acad. Sci. U.S.A. 74*, 2321–2324.

Foundling, S. I., Cooper, J., Watson, F. E., Cleasby, A., Pearl, L. H., Sibanda, B. L., Hemmings, A., Wood, S. P., Blundell, T. L., Valler, M. J., Norey, C. G., Kay, J., Boger, J., Dunn, B. M., Leckie, B. J., Jones, D. M., Atrash, B., Hallet, A., & Szelke, M. (1987) *Nature (London) 327*, 349–352.

Fox, G. C., & Holmes, K. C. (1966) *Acta. Crystallogr. 20*, 886–891.

Gilliland, G. L., Winborne, E. L., Nachman, J., & Wlodawer, A. (1990) *Proteins 8*, 82–101.

Haneef, I., Moss, D. S., Stanford, M. J., & Borkakoti, N. (1985) *Acta. Crystallogr. A41*, 426–433.

James, M. N. G., Sielecki, A. R., Salituro, F., Rich, D. H., & Hofmann, T. (1982) *Proc. Natl. Acad. Sci. U.S.A. 79*, 6137–6142.

Jolles, J., Alais, C., & Jolles, P. (1968) *Biochim. Biophys. Acta 168*, 591–593.

Jones, T. A. (1978) *J. Appl. Crystallogr. 11*, 268–272.

Kabsch, W., & Sander, M. (1983) *Biopolymers 22*, 2577–2637.

Kostka, V. (1985) *Aspartic Proteinases and their Inhibitors*, de Gruyter, West Berlin.

Laemmli, U. K. (1970) *Nature (London) 227*, 680–685.

Lapatto, R., Blundell, T. L., Hemmings, A., Overington, J., Wilderspin, A., Wood, S., Merson, J. R., Whittle, P. J., Danley, D. E., Geoghegan, K. F., Hawrylik, S. J., Lee, S. E., Scheld, K. G., & Hobart, P. M. (1989) *Nature (London) 342*, 299–302.

Mantafounis, D., & Pitts, J. (1990) *Protein Eng. 3*, 605–609.

Marston, F. A. O., Lowe, P. A., Doel, M. T., Schoemaker, J. M., White, S., & Angal, S. (1986) *Bio/Technology 2*, 800–804.

McCamman, M. T., & Cummings, D. B. (1986) *J. Biol. Chem. 261*, 15345–15348.

McCamman, M. T., & Cummings, D. B. (1988) *Proteins 3*, 256–261.

McGregor, M. J., Islam, S. A., & Sternberg, M. J. E. (1987) *J. Mol. Biol. 198*, 295–310.

McPherson, A. (1982) *Preparation and Analysis of Protein Crystals*, J. Wiley & Sons, New York.

McPhie, P. (1976) *Anal. Biochem. 73*, 258–261.

Mercier, J. C., Brington, G., & Ribadeau Dumas, B. (1973) *Eur. J. Biochem. 35*, 222–235.

Messerschmidt, A., & Pflugrath, J. W. (1987) *J. Appl. Crystallogr. 20*, 306–315.

Miller, M., Jaskolski, M., Rao, J. K. M., Leis, J., & Wlodawer, A. (1989) *Nature (London) 337*, 576–579.

Pavlickova, L., et al. (1989) *Collect. Czech. Chem. Commun.* (in press).

Pedersen, V. B., Christensen, K. A., & Foltmann, B. (1979) *Eur. J. Biochem. 94*, 573–580.

Pohl, J., Zaoral, M., Jindra, A., Jr., & Kostka, V. (1984) *Anal. Biochem. 139*, 256–271.

Pohl, J., Strop, P., Pichova, I., Blaha, I., & Kostka, V. (1985) in *Aspartic Proteases and their Inhibitors* (Kostka, V., Ed.) pp 245–264, de Gruyter, West Berlin.

Read, R. J. (1986) *Acta Crystallogr. A42*, 140–149.

Safro, M., Andreeva, N., & Zdanov, A. (1985) in *Aspartic Proteinases and their Inhibitors* (Kostka, V., Ed.) pp 183–187, de Gruyter, West Berlin.

Sali, A., Veerapandian, B., Cooper, J. B., Foundling, S. I., Hoover, D. J., & Blundell, T. L. (1989) *EMBO J. 8*, 2179–2188.

Schechter, I., & Berger, A. (1967) *Biochem. Biophys. Res. Commun. 27*, 157–162.

Sedlacek, J., Fabry, M., & Smrt, J. (1987) *Nucleic Acids, Symp. Ser. 18*, 245–248.

Sibanda, B. L., Blundell, T., Hobart, P. M., Fogliano, M., Bindra, J. S., Dominy, B. W., & Chirgwin, J. M. (1984) *FEBS Lett. 174*, 102–111.

Singh, J., & Thornton, J. M. (1985) *FEBS Lett. 191*, 1–6.

Suguna, K., Padlan, E. A., Smith, C. W., Carlson, W. D., & Davies, D. R. (1987) *Proc. Natl. Acad. Sci. U.S.A. 34*, 7009–7013.

Sutcliffe, M. J., Haneef, I., Carney, D., & Blundell, T. L. (1987) *Protein Eng. 1*, 377–384.

Suzuki, J., Sasaki, K., Sasao, Y., Hamu, A., Kawasaki, H., Nishiyama, M., Horinouchi, S., & Beppu, T. (1989) *Protein Eng. 2*, 563–569.

Tang, J., James, M. N. G., Hsu, I. N., Jenkins, J. A., & Blundell, T. L. (1978) *Nature (London) 271*, 618–621.

Tickle, I. J. (1985) in *Molecular Replacement: Proceedings of the Daresbury Study Weekend* (Machin, P., Ed.) pp 22–26, Daresbury Laboratory, Warrington.

Veerapandian, B., Cooper, J. L., Foundling, S., & Blundell, T. L. (1990) *J. Mol. Biol.* (in press).

Visser, S., Slangen, C. J., & Van Rooijen, P. J. (1987) *Biochem. J. 244*, 553–558.